

Short Note

# *trans*-3-Benzyloxycarbonylamino-1-methyl-3-(methylcarbamoyl)azetidione-1-oxide

Dayi Liu <sup>1</sup>, Régis Guillot <sup>1</sup>, Sylvie Robin <sup>1,2</sup> and David J. Aitken <sup>1,\*</sup>

<sup>1</sup> Université Paris-Saclay, CNRS, ICMMO, 91400 Orsay, France; dayi.liu@universite-paris-saclay.fr (D.L.); regis.guillot@universite-paris-saclay.fr (R.G.); sylvie.robin@universite-paris-saclay.fr (S.R.)

<sup>2</sup> Faculté de Pharmacie, Université Paris Cité, 75006 Paris, France

\* Correspondence: david.aitken@universite-paris-saclay.fr

**Abstract:** *trans*-3-Benzyloxycarbonylamino-1-methyl-3-(methylcarbamoyl)azetidione-1-oxide was prepared by stereoselective oxidation of the corresponding azetidine precursor. The stable molecule was characterized in a low-polarity solution by IR, <sup>1</sup>H-NMR and <sup>13</sup>C-NMR, and in the solid state as a co-crystal with water by X-Ray diffraction. The *N*-oxide function made a strong intramolecular 7-membered ring hydrogen bond with the methyl amide NH in solution and formed an intermolecular H-bond with the carbamate NH in a neighboring molecule in the solid state.

**Keywords:** azetidine; *N*-oxide; hydrogen bonding; crystal structure

## 1. Introduction

*N*-Oxides, traditionally prepared by oxidation of heteroaromatic or tertiary aliphatic amines, are a particular class of organic compounds with distinct chemical and physical properties [1–6]. One of the hallmark features of *N*-oxides is their excellent hydrogen-bond acceptor aptitude. Reports of stable azetidine *N*-oxides are very rare in the literature, due to their intrinsic thermal lability. Oxidation of azetidines is most often followed by fragmentation or rearrangement reactions in mild conditions, without isolation of the *N*-oxides [7–10].

A few notable exceptions have been described by O’Neil, who isolated the azetidine *N*-oxides 1–3 (Figure 1) in moderate yields by treatment of the corresponding azetidines with *m*CPBA [11,12]. Single diastereomers with a *cis* relative configuration were obtained in each case and it was suggested, by analogy with related work conducted on proline derivatives [12–14], that a favorable interaction of *m*CPBA with the substrate’s hydrogen bond donor (acid, alcohol or amide) guided the delivery of the oxygen atom in a *syn* fashion. Compounds 1–3 were reported as stable at room temperature, although alcohol 2 rearranged on heating in CH<sub>2</sub>Cl<sub>2</sub> while peptide 3 decomposed during chromatography on silica. The relative stability of these compounds with respect to other azetidine *N*-oxides was rationalized by 6-membered ring intramolecular hydrogen bonds (Figure 1), which was supported by an X-ray diffraction study on a crystal of 1.

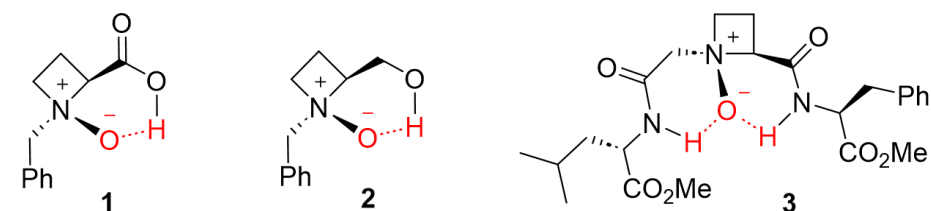


**Figure 1.** Previously described azetidine *N*-oxides and the stabilizing hydrogen bond.

We recently prepared 3-amino-1-methylazetidine-3-carboxylic acid, abbreviated as Aatc(Me), and short peptide derivatives thereof [15–17]. The derivative Cbz-Aatc(Me)-



**Citation:** Liu, D.; Guillot, R.; Robin, S.; Aitken, D.J. *trans*-3-Benzyloxycarbonylamino-1-methyl-3-(methylcarbamoyl)azetidione-1-oxide. *Molbank* **2023**, *2023*, M1726. <https://doi.org/10.3390/M1726>

Received: 24 August 2023

Revised: 10 September 2023

Accepted: 11 September 2023

Published: 15 September 2023

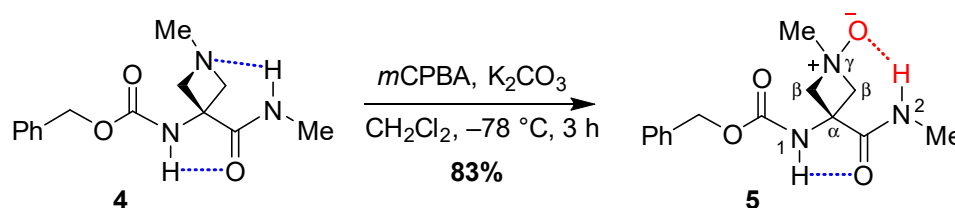


**Copyright:** © 2023 by the authors. Licensee MDPI, Basel, Switzerland. This article is an open access article distributed under the terms and conditions of the Creative Commons Attribution (CC BY) license (<https://creativecommons.org/licenses/by/4.0/>).

NHMe **4** appeared to offer a new opportunity to examine the potential stabilization effects of hydrogen bonding in its corresponding *N*-oxide, so we undertook its preparation and study.

## 2. Results and Discussion

Cbz-Aatc(Me)-NHMe **4** was treated with *m*CPBA in CH<sub>2</sub>Cl<sub>2</sub> solution in mild conditions to furnish the new *N*-oxide *trans*-Cbz-Aatc(Me,O)-NHMe **5** in excellent isolated yield (Scheme 1). The reaction was highly stereoselective, giving only one geometric isomer of product **5**. By analogy with O'Neil's rationale and on the basis of a preferred conformation of **4** implicating the preferred orientation of the methyl amide H-bond donor towards the azetidine lone pair [15], as shown in Scheme 1, we anticipated that the oxygen atom should be delivered in a *syn* manner with respect to the amide, and therefore, a *trans* relative configuration should prevail for **5**.



**Scheme 1.** Synthesis of *trans*-Cbz-Aatc(Me,O)-NHMe **5**. The hydrogen bonds illustrated for both substrate and product are those that prevail in solution.

In low-polarity solvent (CHCl<sub>3</sub>), we obtained evidence for a preferred conformer of **5** with the two intramolecular hydrogen bonds shown in Scheme 1. The IR spectrum showed two absorption bands in the N-H stretch region (Figure 2). The first, centered at 3369 cm<sup>-1</sup>, was assigned to the carbamate NH1, involved in an intra-residue 5-membered ring H-bond. The second was a very broad band, significantly red-shifted to 3245 cm<sup>-1</sup>, that was assigned to the amide NH2, making a strong 7-membered ring H-bond with the azetidine *N*-oxide. No changes were observed in the spectral features over the concentration range 2–30 mM, indicating the intramolecular nature of the H-bonding features.

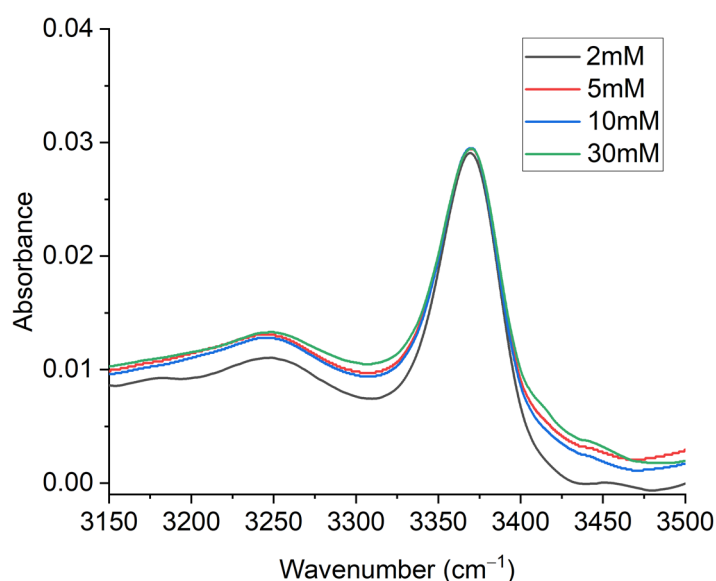


**Figure 2.** IR spectra of compound **5** in CHCl<sub>3</sub> solution at four different concentrations.

<sup>1</sup>H NMR spectroscopic data obtained for **5** in CDCl<sub>3</sub> (5 mM solution) were also revealing. The carbamate NH1 signal appeared noticeably down-field ( $\delta = 6.76$  ppm), in agreement with being involved in a C5 hydrogen bond, whereas the amide NH2 signal

appeared at remarkably low field ( $\delta = 11.60$  ppm), indicating a very strong H-bonding interaction with the *N*-oxide. A DMSO- $d_6$  titration experiment (Figure 3a) revealed very low evolutions in the chemical shifts of the NH signals ( $\Delta\delta = -0.11$  for carbamate NH1 and  $\Delta\delta = -0.21$  for amide NH2, for 10% added DMSO- $d_6$ ), as would be expected for the suggested hydrogen-bonding features. A NOESY experiment (Figure 3b) showed strong correlations between NH2 and both the methyl amide and the *syn* azetidine ring protons (labelled  $\beta$ Hb), while NH1 showed weaker correlations with the  $\beta$ Ha and  $\beta$ Hb protons, in full agreement with the H-bond stabilized conformation represented in Scheme 1.

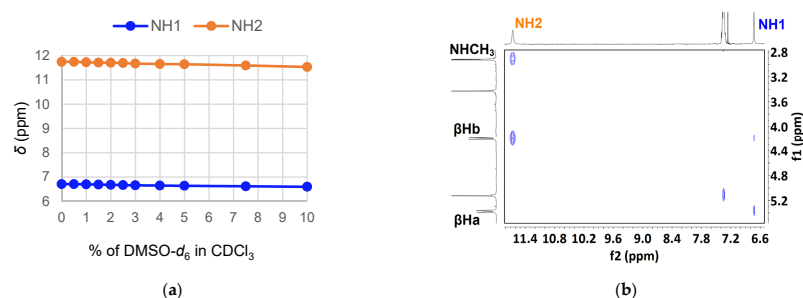


**Figure 3.** (a) Evolution of NH chemical shifts for **5** in the  $\text{CDCl}_3$   $^1\text{H}$  NMR spectrum with incremental addition of DMSO- $d_6$ ; (b)  $^1\text{H}$  NOESY correlations for **5** in  $\text{CDCl}_3$ . The azetidine ring  $\beta$ Ha and  $\beta$ Hb hydrogens are located *syn* with respect to the amino acid NH and the CO groups, respectively.

After unproductive efforts using low-polarity solvents, a single crystal suitable for X-ray diffraction was grown by slow evaporation of a solution in aqueous methanol at room temperature. Compound **5** co-crystallized with water in the triclinic *P*-1 space group with two crystallographically independent molecules in the asymmetric unit. The *trans* relative configuration of **5** was confirmed and a network of intermolecular hydrogen bonds was in evidence in the lattice. The oxygen atom of each azetidine *N*-oxide interacted with the carbamate NH of a neighboring molecule ( $d(\text{O}2\cdots\text{H}6) = 1.90 \text{ \AA}$   $d(\text{O}5\cdots\text{H}3) = 1.87 \text{ \AA}$ ) (Figure 4). The repetition of these interactions within the crystal lattice results in the packing of pairs of waved H-bonded chains running along the *b*-axis, while five ordered water molecules connect the chains through a network of hydrogen bonds (Figure 5). Close contact is observed between each *N*-oxide oxygen atom and a water molecule ( $d(\text{O}2\cdots\text{HOH}) = 1.72 \text{ \AA}$   $d(\text{O}5\cdots\text{HOH}) = 1.98 \text{ \AA}$ ). The adoption of an intermolecular H-bonding regime in the crystal, as opposed to the intramolecular mode evidenced in low-polarity solution, can be attributed to the presence of water as a strong H-bonding network facilitator.

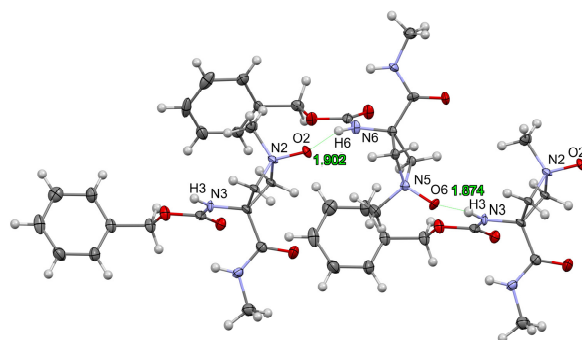


**Figure 4.** X-ray crystal structure of **5** with thermal ellipsoids drawn at a 30% probability level. Water molecules are omitted for clarity. (Note that the amide crystallographic numbering system is different to that used for the isolated molecule presented in Scheme 1).

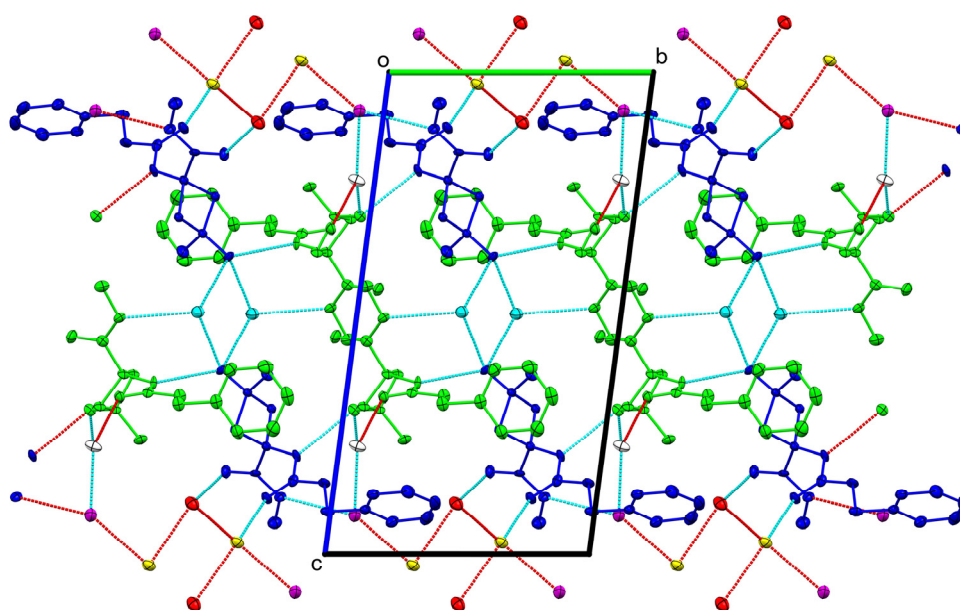


**Figure 5.** View along the a-axis of the hydrogen-bonded chains found in the crystal of compound **5** with moieties colored according to their symmetry equivalence. Water molecules appear in yellow, cyan, magenta, red and white.

The stability of *trans*-Cbz-Aatc(Me,O)-NHMe **5** is noteworthy. It was not degraded during chromatography on silica gel, did not undergo any detectable degradation when stored at room temperature for weeks, and was recovered intact after warming dichloromethane or chloroform solutions to reflux during crystallization attempts. Compound **5** represents a new type of stable azetidine *N*-oxide and we ascribe its stability to its hydrogen-bonding propensity, whether intermolecular in solid state or intramolecular in low-polarity solution.

### 3. Materials and Methods

#### 3.1. General Information

Cbz-Aatc(Me)-NHMe **4** was prepared according to the literature [16]. Commercial *m*-CPBA was purified according to a standard procedure [18]. CH<sub>2</sub>Cl<sub>2</sub> was dried by passage through a column of alumina.

Flash chromatography was performed on silica gel (40–63 μm). The melting point was taken on a Büchi B-540 apparatus in an open capillary tube and was uncorrected. The high-resolution mass spectrum (HRMS [ESI(+)]) was obtained using a Bruker MicrOTOF-Q spectrometer equipped with an electrospray ionization source in positive mode (Figure S2).

Fourier transform infrared (IR) spectra were recorded at 295 K for CHCl<sub>3</sub> solutions held in a Specac Omni-Cell NaCl solution cell (1 mm path length) using a PerkinElmer Spectrum Two spectrometer; maximum absorbances ( $\nu$ ) were reported for significant bands (in cm<sup>-1</sup>).

<sup>1</sup>H and <sup>13</sup>C NMR spectra were recorded at 300 K in CDCl<sub>3</sub> solution on a Bruker spectrometer operating at 400 MHz (for <sup>1</sup>H) or at 100 MHz (for <sup>13</sup>C). Chemical shifts ( $\delta$ ) were reported in parts per million (ppm) with respect to residual protonated solvent ( $\delta$  = 7.26 ppm) for <sup>1</sup>H and the deuterated solvent ( $\delta$  = 77.16 ppm) for <sup>13</sup>C. Splitting patterns for <sup>1</sup>H signals were designated as s (singlet), d (doublet), m (multiplet), or bs (broad singlet); coupling constants ( $J$ ) were reported in hertz. For the DMSO-*d*<sub>6</sub> titration experiment, a sample was dissolved in CDCl<sub>3</sub> (400 μL) to give a 5 mM solution. Aliquots of DMSO-*d*<sub>6</sub> (6 × 2 μL, 2 × 4 μL, 2 × 10 μL) were added successively to the NMR tube and the spectrum was re-recorded after each addition. For the NOESY experiment (20 mM in CDCl<sub>3</sub>), the pulse sequence was noesygpqh, collecting 2048 points in f2 and 256 points in f1, and the mixing time was 600 ms.

### 3.2. Synthesis of *trans*-Cbz-Aatc(Me,O)-NHMe, 5

A solution of Cbz-Aatc(Me)-NHMe **4** (28 mg, 0.1 mmol, 1 eq.) in dry CH<sub>2</sub>Cl<sub>2</sub> (4 mL) under an argon atmosphere was cooled to −78 °C. Potassium carbonate (28 mg, 0.2 mmol, 2 eq.) and *m*-CPBA (21 mg, 0.1 mmol, 1 eq.) were added successively. The mixture was stirred at −78 °C for 3 h then allowed to warm to room temperature. The suspension was filtered through a 0.45 μm PTFE membrane, and the filtrate was collected and evaporated under reduced pressure. The crude product was purified by flash chromatography (CH<sub>3</sub>CN:MeOH:NH<sub>4</sub>OH (28% aq.), gradient from 20:20:1 to 20:20:2) to give **5** as a white solid (24 mg, 83%). *R*<sub>f</sub> = 0.21 (CH<sub>3</sub>CN:MeOH:NH<sub>4</sub>OH = 20:20:1). *M*<sub>p</sub> = 149–151 °C (dec.) <sup>1</sup>H NMR (400 MHz, CDCl<sub>3</sub>) δ 11.61 (bs, 1H, NH<sup>2</sup>), 7.42–7.31 (m, 5H, CH<sup>Ar</sup>), 6.76 (bs, 1H, NH<sup>1</sup>), 5.38 (d, *J* = 11.6 Hz, 2H, C<sup>β</sup>H<sup>a</sup>), 5.13 (s, 2H, CH<sub>2</sub><sup>Cbz</sup>), 4.22 (d, *J* = 11.6 Hz, 2H, C<sup>β</sup>H<sup>b</sup>), 3.43 (s, 3H, N<sup>γ</sup>CH<sub>3</sub>), 2.92 (d, *J* = 4.5 Hz, 3H, N<sup>2</sup>CH<sub>3</sub>). <sup>13</sup>C NMR (100 MHz, CDCl<sub>3</sub>) δ 170.34 (CO), 155.06 (CO), 135.97 (C<sup>Ar</sup>), 128.79, 128.52, 128.04 (CH<sup>Ar</sup>), 77.65 (C<sup>β</sup>H<sub>2</sub>), 67.00 (CH<sub>2</sub><sup>Cbz</sup>), 58.51 (N<sup>γ</sup>CH<sub>3</sub>), 51.75 (C<sup>α</sup>), 26.97 (N<sup>2</sup>CH<sub>3</sub>). IR (CHCl<sub>3</sub>) ν 3369, 3245br, 2923, 2854, 1698, 1670, 1574, 1537 cm<sup>−1</sup>. HRMS [ESI(+)] *m/z* [M+H]<sup>+</sup> calculated for [C<sub>14</sub>H<sub>20</sub>N<sub>3</sub>O<sub>4</sub>]<sup>+</sup>: 294.1448, found: 294.1441.

### 3.3. Single Crystal XRD Study of 5

X-ray diffraction data were collected using a VENTURE PHOTON II c14 Bruker diffractometer with Micro-focus IμS source Mo Kα radiation. A crystal was mounted on a CryoLoop (Hampton Research) with Paratone-N (Hampton Research) as cryoprotectant and then flash-frozen in a nitrogen gas stream at 200 K. The temperature of the crystal was maintained (within an accuracy of ±1 K) by means of a 700 series Cryostream cooling device. Data were corrected for Lorentz polarization and absorption effects. The structure was solved by direct methods using SHELXT-2018 [19] and refined against *F*<sup>2</sup> by full-matrix least-squares techniques using SHELXL-2019 [20] with anisotropic displacement parameters for all non-hydrogen atoms. Hydrogen atoms were located on a difference Fourier map and introduced into the calculations as a riding model with isotropic thermal parameters. All calculations were performed by using the Crystal Structure crystallographic software package WinGX [21].

Crystal data for **5**: 2(C<sub>14</sub>H<sub>19</sub>N<sub>3</sub>O<sub>4</sub>)·5(H<sub>2</sub>O) (*M*<sub>r</sub> = 676.72 g·mol<sup>−1</sup>) triclinic, *P*-1 (No. 2), *a* = 9.5365(4) Å, *b* = 10.4289(3) Å, *c* = 18.2694(7) Å, α = 96.9320(10)°, β = 90.811(2)°, γ = 108.3310(10)°, *V* = 41,709.56(11) Å<sup>3</sup>, *T* = 200(1) K, *Z* = 2, *Z*' = 1, μ(Mo Kα) = 0.104 mm<sup>−1</sup>, 11,378 reflections measured, 1361 unique (*R*<sub>int</sub> = 0.0777), which were used in all calculations. The final *wR*<sub>2</sub> was 0.0847 (all data) and *R*<sub>1</sub> was 0.0353 (*I* > 2σ(*I*)).

**Supplementary Materials:** The following are available online: <sup>1</sup>H and <sup>13</sup>C NMR spectra (Figure S1), HRMS spectrum (Figure S2).

**Author Contributions:** Conceptualization, methodology, project administration: D.J.A.; data acquisition: D.L. and R.G.; supervision and validation: S.R. and D.J.A.; writing: all authors. All authors have read and agreed to the published version of the manuscript.

**Funding:** D.L. is the awardee of a China Scholarship Council PhD grant.

**Data Availability Statement:** CCDC 2284861 contains the supplementary crystallographic data for compound **5**. These data can be obtained free of charge via [www.ccdc.cam.ac.uk/data\\_request/cif](http://www.ccdc.cam.ac.uk/data_request/cif), by emailing [data\\_request@ccdc.cam.ac.uk](mailto:data_request@ccdc.cam.ac.uk), or by contacting the Cambridge Crystallographic Data Center, 12 Union Road, Cambridge CB2 1EZ, UK, fax: +44-1223-33603.

**Acknowledgments:** The authors acknowledge the ICMMO Mass Spectrometry service for recording the HRMS spectrum.

**Conflicts of Interest:** The authors declare no conflict of interest.

## References

1. Habib, I.; Singa, K.; Hossain, M. Recent Progress on Pyridine *N*-Oxide in Organic Transformations: A Review. *Chem. Select* **2023**, *8*, e202204099. [[CrossRef](#)]
2. Fershtat, L.L.; Tesenko, F.E. Five-Membered Heterene *N*-Oxides: Recent Advances in Synthesis and Reactivity. *Synthesis* **2021**, *53*, 3673–3682. [[CrossRef](#)]
3. Wrzeszcz, Z.; Siedlecka, R. Heteroaromatic *N*-Oxides in Asymmetric Catalysis: A Review. *Molecules* **2020**, *25*, 330. [[CrossRef](#)] [[PubMed](#)]
4. Bernier, D.; Wefelscheid, U.K.; Woodward, S. Properties, Preparation and Synthetic Uses of Amine *N*-Oxides. An Update. *Org. Prep. Proced. Int.* **2009**, *41*, 173–210. [[CrossRef](#)]
5. O'Neil, I.A. Product Class 3: Amine *N*-Oxides. In *Science of Synthesis*; Schaumann, E., Ed.; Thieme: Stuttgart, Germany, 2008; Volume 40b, pp. 855–891.
6. Albini, A. Synthetic Utility of Amine *N*-Oxides. *Synthesis* **1993**, *1993*, 263–277. [[CrossRef](#)]
7. Menguy, L.; Drouillat, B.; Marrot, J.; Couty, F. Mechanistic Insights into the Rearrangement of Azetidene *N*-oxides to Isoxazolidines. *Tetrahedron Lett.* **2012**, *53*, 4697–4699. [[CrossRef](#)]
8. Yoneda, R.; Araki, L.; Harusawa, S.; Kurihara, T. Studies on the [2,3]-Meisenheimer Rearrangement of 2-Vinylazetidene *N*-Oxides. *Chem. Pharm. Bull.* **1998**, *46*, 853–856. [[CrossRef](#)]
9. Kurihara, T.; Sakamoto, Y.; Tsukamoto, K.; Ohishi, H.; Harusawa, S.; Yoneda, R. Meisenheimer Rearrangement of Azetopyridinoides. Part 4. Ring Expansion of 2-Vinyl-1,2,4,10,10a-hexahydroazeto[1',2':1,2]pyrido[3,4-*b*]indole *N*-oxides. *J. Chem. Soc. Perkin Trans. 1* **1993**, *1993*, 81–87. [[CrossRef](#)]
10. Kurihara, T.; Sakamoto, Y.; Takai, M.; Ohuchi, K.; Harusawa, S.; Yoneda, R. Meisenheimer Rearrangement of Azetopyridinoides. III. Synthesis of 3,6-Epoxyhexahydroazocino[5,4-*b*]indoles. *Chem. Pharm. Bull.* **1993**, *41*, 1221–1225. [[CrossRef](#)]
11. O'Neil, I.A.; Potter, A.J. Simple Azetidene *N*-Oxides: Synthesis, Structure and Reactivity. *Chem. Commun.* **1998**, *1998*, 1487–1488. [[CrossRef](#)]
12. O'Neil, I.A.; Miller, N.D.; Barkley, J.V.; Low, C.M.R.; Kalindjian, S.B. Homochiral Proline *N*-Oxides as Conformational Constraints in Proline Like Molecules. *Synlett* **1995**, *1995*, 619–621. [[CrossRef](#)]
13. O'Neil, I.A.; Miller, N.D.; Barkley, J.V.; Low, C.M.R.; Kalindjian, S.B. The Synthesis of Proline Derived Homochiral Amine Oxides. *Synlett* **1995**, *1995*, 617–618. [[CrossRef](#)]
14. O'Neil, I.A.; Miller, N.D.; Peake, J.; Barkley, J.V.; Low, C.M.R.; Kalindjian, S.B. The Novel Use of Proline Derived Amine Oxides in Controlling Amide Conformation. *Synlett* **1993**, *1993*, 515–518. [[CrossRef](#)]
15. Mundlapati, V.R.; Imani, Z.; D'mello, V.C.; Brenner, V.; Gloaguen, E.; Baltaze, J.-P.; Robin, S.; Mons, M.; Aitken, D.J. N-H...X interactions stabilize intra-residue C5 hydrogen bonded conformations in heterocyclic  $\alpha$ -amino acid derivatives. *Chem. Sci.* **2021**, *12*, 14826–14832. [[CrossRef](#)] [[PubMed](#)]
16. Liu, D.; Imani, Z.; Gourson, C.; Guillot, R.; Robin, S.; Aitken, D.J. A Post-Synthetic Modification Strategy for the Preparation of Homooligomers of 3-Amino-1-methylazetidene-3-carboxylic acid. *Synlett* **2023**, *34*, 1787–1790. [[CrossRef](#)]
17. Liu, D.; Bardaud, J.-X.; Imani, Z.; Robin, S.; Gloaguen, E.; Brenner, V.; Aitken, D.J.; Mons, M. Length-Dependent Transition from Extended to Folded Shapes in Short Oligomers of an Azetidene-Based  $\alpha$ -Amino Acid: The Critical Role of NH...N H-Bonds. *Molecules* **2023**, *28*, 5048. [[CrossRef](#)] [[PubMed](#)]
18. Perrin, D.D.; Armarego, W.L.F. *Purification of Laboratory Chemicals*, 3rd ed.; Pergamon: Oxford, UK, 1988; p. 123.
19. Sheldrick, G.M. SHELXT—Integrated space-group and crystal-structure determination. *Acta Cryst.* **2015**, *A71*, 3–8. [[CrossRef](#)] [[PubMed](#)]
20. Sheldrick, G.M. Crystal structure refinement with SHELXL. *Acta Cryst.* **2015**, *C71*, 3–8.
21. Farrugia, L.J. WinGX suite for small-molecule single-crystal crystallography. *J. Appl. Cryst.* **1999**, *32*, 837–838. [[CrossRef](#)]

**Disclaimer/Publisher's Note:** The statements, opinions and data contained in all publications are solely those of the individual author(s) and contributor(s) and not of MDPI and/or the editor(s). MDPI and/or the editor(s) disclaim responsibility for any injury to people or property resulting from any ideas, methods, instructions or products referred to in the content.